Dielectrophoresis based discrimination of human embryonic stem cells from differentiating derivatives

Srinivas Velugotla, Steve Pells, Heidi K. Mjoseng, Cairnan R. E. Duffy, Stewart Smith, Paul De Sousa, and Ronald Pethig

Citation: Biomicrofluidics **6**, 044113 (2012); doi: 10.1063/1.4771316
View online: http://dx.doi.org/10.1063/1.4771316
View Table of Contents: http://scitation.aip.org/content/aip/journal/bmf/6/4?ver=pdfcov
Published by the AIP Publishing

Dielectrophoresis based discrimination of human embryonic stem cells from differentiating derivatives

Srinivas Velugotla,[1] Steve Pells,[2] Heidi K. Mjoseng,[2] Cairnan R. E. Duffy,[2] Stewart Smith,[1] Paul De Sousa,[2,a),b)] and Ronald Pethig[1,a),b)]
[1]*Institute for Integrated Micro and Nano Systems, School of Engineering, The University of Edinburgh, Edinburgh EH9 3JF, United Kingdom*
[2]*Centre for Regenerative Medicine, College of Medicine and Veterinary Medicine, The University of Edinburgh, Chancellor's Building, Edinburgh EH16 4SB, United Kingdom*

(Received 24 August 2012; accepted 27 November 2012; published online 12 December 2012)

Assessment of the dielectrophoresis (DEP) cross-over frequency (f_{xo}), cell diameter, and derivative membrane capacitance (C_m) values for a group of undifferentiated human embryonic stem cell (hESC) lines (H1, H9, RCM1, RH1), and for a transgenic subclone of H1 (T8) revealed that hESC lines could not be discriminated on their mean f_{xo} and C_m values, the latter of which ranged from 14 to 20 mF/m^2. Differentiation of H1 and H9 to a mesenchymal stem cell-like phenotype resulted in similar significant increases in mean C_m values to 41–49 mF/m^2 in both lines ($p < 0.0001$). BMP4-induced differentiation of RCM1 to a trophoblast cell-like phenotype also resulted in a distinct and significant increase in mean C_m value to 28 mF/m^2 ($p < 0.0001$). The progressive transition to a higher membrane capacitance was also evident after each passage of cell culture as H9 cells transitioned to a mesenchymal stem cell-like state induced by growth on a substrate of hyaluronan. These findings confirm the existence of distinctive parameters between undifferentiated and differentiating cells on which future application of dielectrophoresis in the context of hESC manufacturing can be based. © *2012 American Institute of Physics*. [http://dx.doi.org/10.1063/1.4771316]

I. INTRODUCTION

Human embryonic stem cells (hESCs) isolated from early blastocyst stage embryos[1,2] and comparably pluripotent stem cells induced from adult cells by gene transduction[3] (iPSCs) constitute a promising resource for disease modeling, drug screening, and cell therapies for regenerative medicine. This is found on their immortality and pluripotency, as compared to the restricted growth potential and repertoires of adult tissue-sourced stem cells. However, the breadth of this capacity also makes controlling cell behavior *in vitro* more difficult, potentially undermining their utility due to variable and heterogeneous cell production and the difficulty of distinguishing cells of a desired phenotype from other contaminating populations. Thus, to achieve standardized production of the quantity and type of cells desired for particular applications, there is a need for sensitive and non-invasive methods to discriminate and ultimately segregate live cell populations.

Dielectrophoresis (DEP) is a well studied electrokinetic technique[4–7] which has been used to discriminate between distinct cellular identities in heterogeneous populations, notably haematopoietic stem cells and differentiated derivatives in bone marrow and blood,[8,9] mesenchymal stem cells in adipose tissue,[10] and neural stem cell populations.[11,12] A DEP device for antibody-independent capture of viable circulating cancer cells in blood has already been developed,[13] and theoretically DEP could provide a simple and non-invasive way to

a)Authors to whom correspondence should be addressed. Electronic addresses: Paul.Desousa@ed.ac.uk and Ron.Pethig@ed.ac.uk.
b)P. De Sousa and R. Pethig contributed equally to this work.

positively or negatively select for target or contaminating cell types in a cell preparation intended for transplantation. The DEP response of a cell involves either movement up a field gradient towards an electrode (positive DEP) or down a field gradient away from an electrode (negative DEP). A transition between these two responses occurs where the effective polarisability of the cell matches that of the surrounding medium, and this can occur at both a low frequency (kHz range) or high frequency (>100 MHz). In the kHz range explored in this work, the corresponding DEP cross-over frequency f_{xo} for a spherical cell of radius r is given to good approximation by

$$f_{xo} = \frac{\sqrt{2}\sigma_m}{2\pi r C_m}, \tag{1}$$

where C_m is the specific capacitance of the cell membrane and σ_m is the conductivity of the suspending medium.[7]

Measurement of f_{xo} and C_m has been shown to provide a sensitive, non-invasive way to monitor changes in cell states associated with activation and clonal expansion, apoptosis, necrosis, and responses to chemical and physical agents.[14–17] As such, DEP could be applied in the context of stem cell processing as a means for real-time characterisation of the identity and viability of manufactured cell preparations.

Recently, the application of DEP to neural stem cell populations suggested that the differentiation fate of neural stem cells could be predicted by distinct changes in their f_{xo} and C_m values before the presence of specific cell-surface proteins (antigens) could be detected.[12,13] In the present study, our objective was to evaluate DEP as a means to discriminate and characterize undifferentiated hESCs and differentiating progeny. This is an important prerequisite to an ambition to use DEP in the context of manufacturing hESC derived cell products given variation which can exist between cell lines in the course of adaptation to culture or genetic modification. Using the aforementioned Eq. (1), we measured f_{xo} and derive C_m values in several undifferentiated hESC lines (H1, H9, RCM1, RH1),[1,18–20] a transgenic clonal derivative (T8; a subclone of H1 expressing a genome-integrated green fluorescent protein (GFP) reporter under the control of the OCT4-pluripotency associated transcription factor promoter),[20] and derivatives of these cell lines to multipotent-mesenchymal-stem cell like cells[21] and to trophoblast.[22] Our findings confirm the existence of distinctive parameters of undifferentiated and differentiating cells on which future application of DEP in hESC manufacturing can be based.

II. MATERIALS AND METHODS

A. Cell culture

The use of hESC lines in this project was approved by the MRC steering committee overseeing the UK Stem Cell Bank. RCM1 and RH1 were derived at the Roslin Institute under a license from the Human Fertilisation and Embryology Authority to P. De Sousa and licensed from Roslin Cells and Geron, respectively. Both cell lines have been deposited in the UKSCB (www.ukstemcellbank.org.uk). H1 and H9 were derived first at Wisconsin Regional Primate Research Center, University of Wisconsin and licensed from WiCell. They are available from the Wisconsin International Stem Cell Bank (www.wicell.org). The T8 cell line was derived at the Roslin Institute by transfecting the H1 hESC cell line with an octamer-binding transcription factor 4-GFP (OCT4-GFP) reporter.

RCM1,[18] RH1,[19] H1 and H9,[1] and T8 (Ref. 20) hESCs were cultured on plastic tissue culture plates (Corning Inc., NY) coated with growth factor-reduced Matrigel™ (Becton Dickinson) at 37 °C, 5% CO_2. T8 hESCs were cultured in mTeSR1 medium (Stemcell Technologies) supplemented with 100 μg ml^{-1} G418 (Gibco).[20] RCM1, RH1, H1, and H9 hESCs were cultured in mTeSR1 alone. Cells were routinely passaged using 200 units/ml of collagenase in Knockout Dulbecco's modified Eagle medium (KO-DMEM, Invitrogen) followed by manual scraping.

H1 and H9 hESCs were differentiated to a mesenchymal stem cell like phenotype using an established protocol involving successive passaging on a substrate of hyaluronan (HA), also

known as hyaluronic acid or hyaluronate,[21] in a human dermal fibroblast conditioned medium (HDF-CM) composed of KO-DMEM, 20% knockout serum replacement (KOSR, Invitrogen), 1 mM glutamine, 0.1 mM β-mercaptoethanol, and 4 ng/ml bFGF, prepared as described previously.[17] Mesenchymal stem cell-like lines originating from H1 and H9 were designated H1-MSC and H9-MSC, respectively. A stock solution of hyaluronan (1200 kD, Proud.385908, Merck-Calbiochem, Nottingham, UK) was produced by solubilising it in physiological strength phosphate buffered saline (PBS) at 10 mg/ml and used for substrate coating. Tissue culture wells were coated with HA stock solution applied at 0.1 ml/cm^2 for 30 min at 4 °C before warming to room temperature and grown in 80% KO-DMEM and 20% KOSR (Gibco). For trophoblast cell differentiation, RCM1 hESCs were cultured on Matrigel™ (Becton Dickinson) coated plastic tissue culture plates in HDF-CM (Ref. 18) further supplemented with bone morphogenetic protein (BMP4) at 100 ng/ml for 7 days as described previously.[22] These cells were designated RCM1-trophoblast.

For immunolabeling, both hESCs and differentiated cells were washed in PBS buffer and fixed with 4% paraformaldehyde (PFA), permeabilised with 0.2% igepal (Sigma), and blocked in 10% rabbit serum (Millipore). Fixed and permeabilised hESCs were incubated with mouse anti-OCT4 (dilution 1:50, Santa Cruz Biotechnology). Primary antibody binding was detected by incubating with rabbit anti-mouse Alexa-Fluor®-488 (dilution 1:200, Invitrogen); nuclei were counterstained with DAPI[23] (Roche). Fixed and permeabilised HA-differentiated cells were washed in PBS and stained to detect mesenchymal markers by incubating with goat anti-human CD105 (1:50 dilution, R&D Systems), and mouse anti-human STRO-1 (1:200 dilution, Millipore). Secondary antibodies were donkey anti-goat Alexa-Fluor-555 (1:400 dilution, Invitrogen), and rabbit anti-mouse Alexa-Fluor-488 (1:200 dilution, Invitrogen), respectively. Fixed and permeabilised RCM1-trophoblast cells were washed in PBS and incubated with mouse anti-human CDX2 (1:50 dilution, Vector labs) and mouse anti-hCG-β (1:25 dilution, Abcam). Primary antibodies were detected by incubating with goat anti-mouse Alexa-Fluor-488 (dilution 1:200, Invitrogen) and nuclei were counterstained with DAPI[23] (Roche). Images were captured with a Zeiss Observer microscope and Nikon camera.

B. Osteoblast formation

Osteogenic differentiation was induced as previously described by Sottile *et al.*[24] An osteogenic (OS) supplement consisting of 50 μM ascorbic acid phosphate (Wako, Neuss, Germany), 10 mM β-glycerophosphate (Sigma-Aldrich, Dorset, UK), and 100 nM dexamethasone (Sigma-Aldrich, Dorset, UK) was added to DMEM medium. Cells grown previously on HA (H1) for 10 passages were plated on 0.1% gelatin and treated with embryoid body differentiation (EBD) medium consisting of 80% KO-DMEM (Invitrogen), 20% fetal bovine serum (FBS) (PAA Laboratories, Pasching, Austria), 1 mM L-glutamine, 0.1 mM μ-mercaptoethanol, 1% nonessential amino acids (all Invitrogen) +/− OS that was changed every 2 days over the indicated intervals.

1. Mineralisation analysis

For mineralized nodule detection, fixed wells of cells were washed twice with calcium and magnesium-free (CMF)-PBS before incubation with a 1% Alizarin-Red S (Sigma-Aldrich, Dorset, UK) solution in CMF-PBS for 10 min. This was followed by washing twice with water and then fixation in 95% methanol. Cell matrix-associated calcium deposition was determined in 96-well plates using the Sigma calcium assay kit (Sigma-Aldrich, Dorset, UK), in triplicate wells.

C. Flow cytometry

Single cell suspensions of cultured cells were prepared by treatment with Trypsin-EDTA (Gibco Invitrogen, Paisley, UK) for 5–10 min at 37 °C followed by re-suspension in FACS PBS (PBS with 0.1% bovine serum albumin [BSA]). Cells were incubated for 20 min at 4 °C with pre-conjugated MSC markers CD73-PE (BD Biosciences), CD105-FITC, CD90-FITC, Stro1-

APC, CD34-PE (BD Biolegend), and CD14-PE (Becton Dickson). To remove unbound antibody, 2 ml of FACS PBS were added per aliquot, and decanted after centrifugation at (1300 rpm) for 5 min. Cell samples finally resuspended in 250 μl FACS PBS and analyzed using a flow cytometer (FACSCalibur Becton Dickinson) equipped with 488 nm and 633 nm lasers and standard filter set. FACS data were analyzed and plotted using FCS EXPRESS software.

D. DEP studies

DEP cross-over frequencies f_{xo} for individual cells were obtained using the electrode design shown in Figure 1. The electrodes were fabricated using standard photolithography and liftoff techniques, and consisted of gold (150 nm) thermally evaporated onto a chrome adhesion layer (5 nm) and patterned into an interdigitated array on a glass substrate. The electrode substrate formed the floor of an open chamber, of internal length 10 mm, width 10 mm, and height 80 μm, constructed from polydimethylsiloxane (PDMS) bonded onto the glass substrate containing the electrodes. The spatial variation of the field non-uniformity generated by this interdigitated electrode design, characterized by the factor ∇E^2, was modeled using COMSOL (Multiphysics 4.3) finite element software. This information was used to derive the magnitude of the DEP force acting on typical cells as a function of the applied sinusoidal voltage and location above the electrode plane.

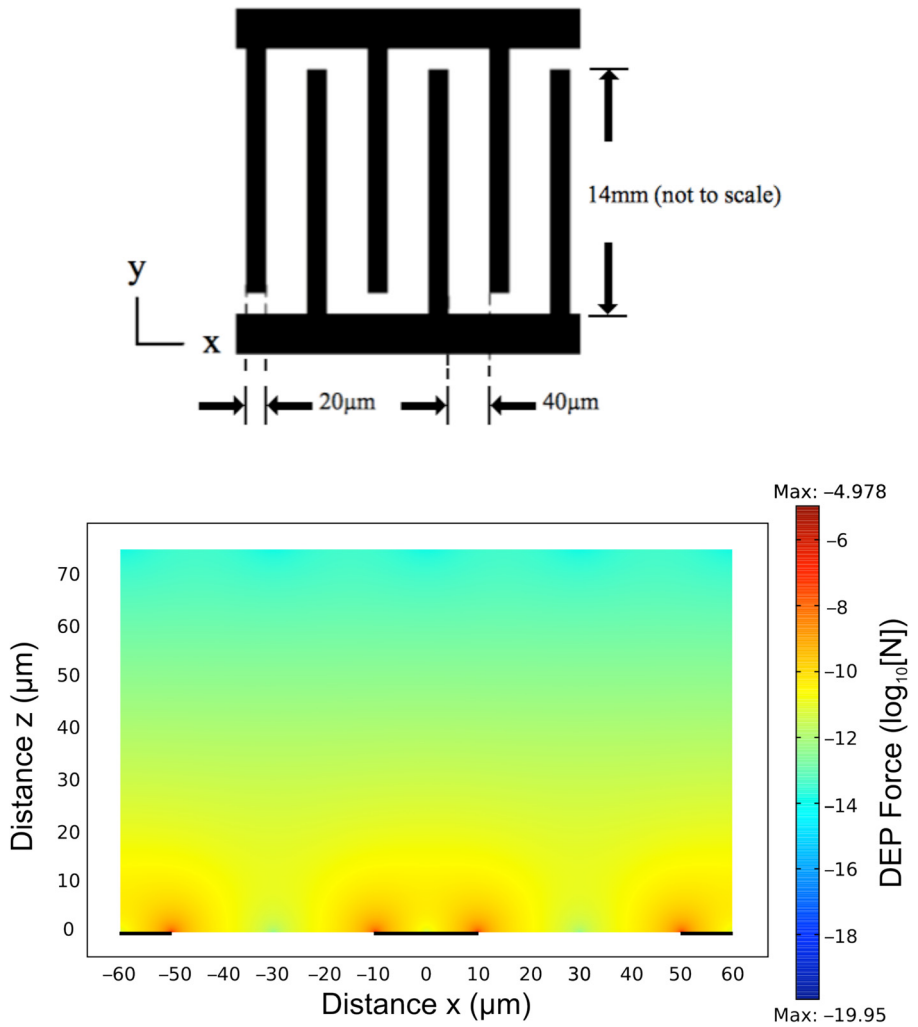

FIG. 1. (Top): Interdigitated electrode geometry used to determine the DEP cross-over frequency f_{xo}. (Bottom): COMSOL Multiphysics simulation of the DEP force ($\log_{10}$[N]) acting on a 10 μm diameter cell (Clausius-Mossotti factor = 0.5) with an applied voltage of 3 V (pk), as a function of distance (x μm) along and height above (z μm) the electrode plane.

An example of this modelling is shown in Figure 1. The maximum Brownian diffusional force ($kT/2r$) acting on a cell of radius 5 μm at room temperature is 4×10^{-16} N, and from Figure 1, the corresponding DEP force for an applied voltage of 3 V(pk) greatly exceeded this value. However, the sedimentation force acting on a 5 μm radius cell can be estimated as 2×10^{-13} N (assuming a specific density difference of 40 kg/m^3 between the medium and cell). To ensure that sedimentation forces did not influence the assessment of the DEP force when close to f_{xo}, studies were limited to those cells located no higher than 20 μm above the electrode plane.

Before DEP characterization the cells were centrifuged ($100\times g$, 5 min) and washed twice in 10 ml of the DEP medium, before final suspension in this medium at a density of $\sim 10^7$ cells/ml. The DEP isotonic medium consisted of 8.5% (w/w) sucrose, 0.5% (w/w) glucose, at pH 7.4 (adjusted with NaOH) and conductivity 33 mS/m, adjusted with PBS. Osmolality (310 mOsm) and conductivity values were measured using an osmometer (Advanced Instruments Inc., Model 3300) and a conductivity meter (Oakton CON 510), respectively. Cell suspensions were pipetted onto the electrodes, the chamber was closed with a cover slip and then mounted in an inverted microscope (Meiji TC5100). Sinusoidal voltages of 3 V (pk) were applied to the electrodes in continuous incremental steps of 10 kHz, commencing at 10 kHz and finishing at 200 kHz, using an Agilent/HP 3325 A signal generator. By focusing on the electrode plane discrimination between cells undergoing negative DEP and positive DEP was possible, and an estimation of f_{xo} was made for each cell by analysis of video images captured during this procedure. The diameter of each characterized cell was measured using Free Ruler (www.pascal.com/software/freeruler).

E. Statistical analysis

Statistical analyses (unpaired t-tests or one-way ANOVA with Tukey's post-hoc test, as appropriate) were performed in GraphPad Prism, version 6.

III. RESULTS AND DISCUSSION

The undifferentiated phenotype and pluripotency of hESC lines used in this study has been reported in previous studies.[1,18–20] Flow cytometry confirmed all lines were positive for undifferentiated glycolipids SSEA-4 and TRA-1-60, and negative for SSEA-1 (Table I). The former were lower in the transgenic GFP reporter-expressing T8 line. By *in situ* immunocytochemistry undifferentiated cell colonies in all lines were positive for pluripotency associated transcription factors, Oct4 and Nanog (Oct4 shown for H1, Figure 2(a)). H1 and H9 hESC's were differentiated to MSC-like lineages as previously reported in Harkness *et al.*[21] Consistent with an adult tissue derived MSC flow cytometry confirmed cells were CD73+, CD105+, CD90+, and Stro1+ and CD14−, CD34− (shown for H1, Figure 3). CD105 and Stro1 expression was confirmed by immunocytochemistry (Figure 2(b)). To confirm a MSC-like potency, cells were induced to undergo mineralization *in vitro* in response to an osteogenic stimulus (OS) as previously described by Sottille *et al.*[24] H1-MSC grown on HA for 10 passages underwent OS

TABLE I. Flow cytometry analysis data for five undifferentiated hESC lines used in the study confirmed that comparable and high level of detection of SSEA-4 and TRA-1-60 and low levels of SSEA-1, as expected for this phenotype. Passage number at which cells assessed denoted by "p."

	% marker positive		
hESC lines	SSEA-1	SSEA-4	TRA1-60
H1-p62	4	69	63
H9-p73	2	85	75
RCM1-p65	5	97	97
RH1-p53	5	60	71
T8-p98	3	32	66

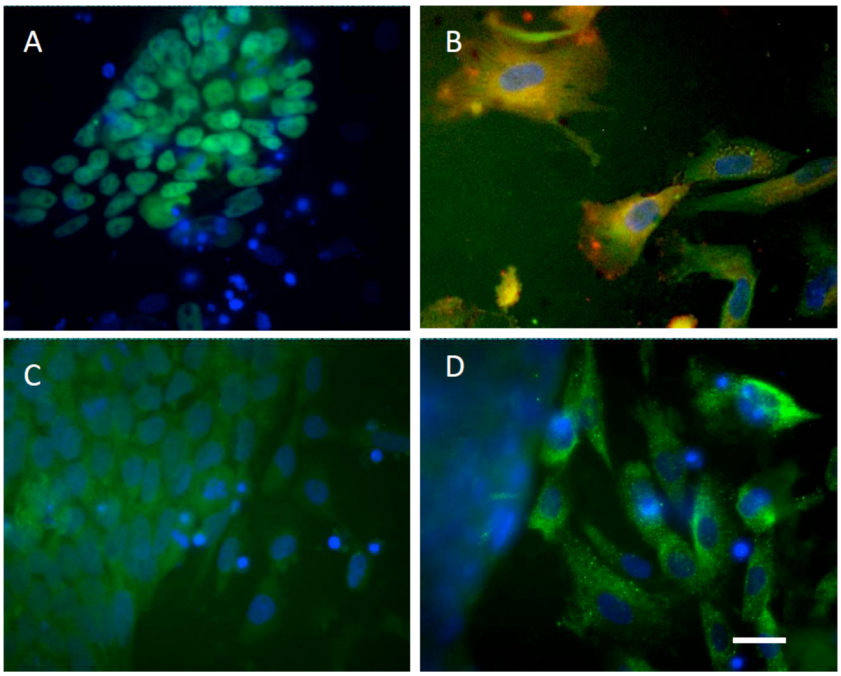

FIG. 2. Immunocytochemical confirmation of hESC and derivative lineages. Undifferentiated H1 hESCs (a) and MSC-like cells (b), and RCM-1 trophoblast-like cells ((c), (d)) stained for OCT4 (a), MSC lineage markers CD105 (red) and Stro-1 (green) (b) and trophoblast markers CDX2 (green, (c)) and hCG-β (green, (d)). Nuclei are counterstained with DAPI (blue) in all panels. Scale bar equals to 20 μm.

dependent mineralization characteristic of osteoblast-like cells. This was reflected by Alazarin Red staining and calcium deposition (Figure 4), both of which increased over successive days of stimulation and were maximal by 10 days of treatment respectively. RCM1 cells were non-specifically differentiated to yield heterogeneous populations of trophoblast like cells using another established protocol Xu *et al.*[22] This was verified by immunostaining for CDX2 and hCG-β markers (Figures 2(c) and 2(d)).

A summary of the experimentally measured cell diameters and DEP cross-over frequencies (f_{xo}) for the various hESCs and their differentiated progeny is given in Table II, together with

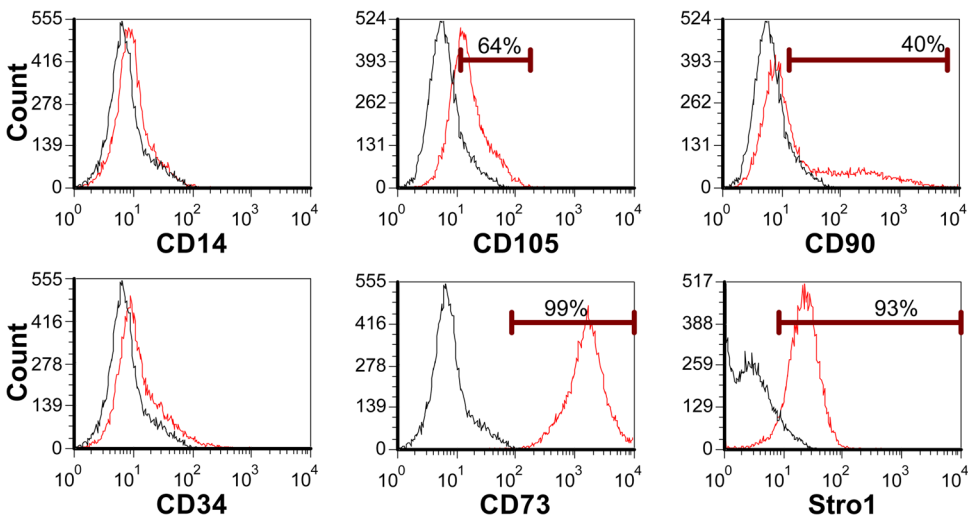

FIG. 3. Flow cytometric analysis of H1-MSC-like cells confirmed they were negative for CD14, CD34, and positive for CD105 (64%), CD90 (40%), CD73 (99%), and Stro1 (58%).

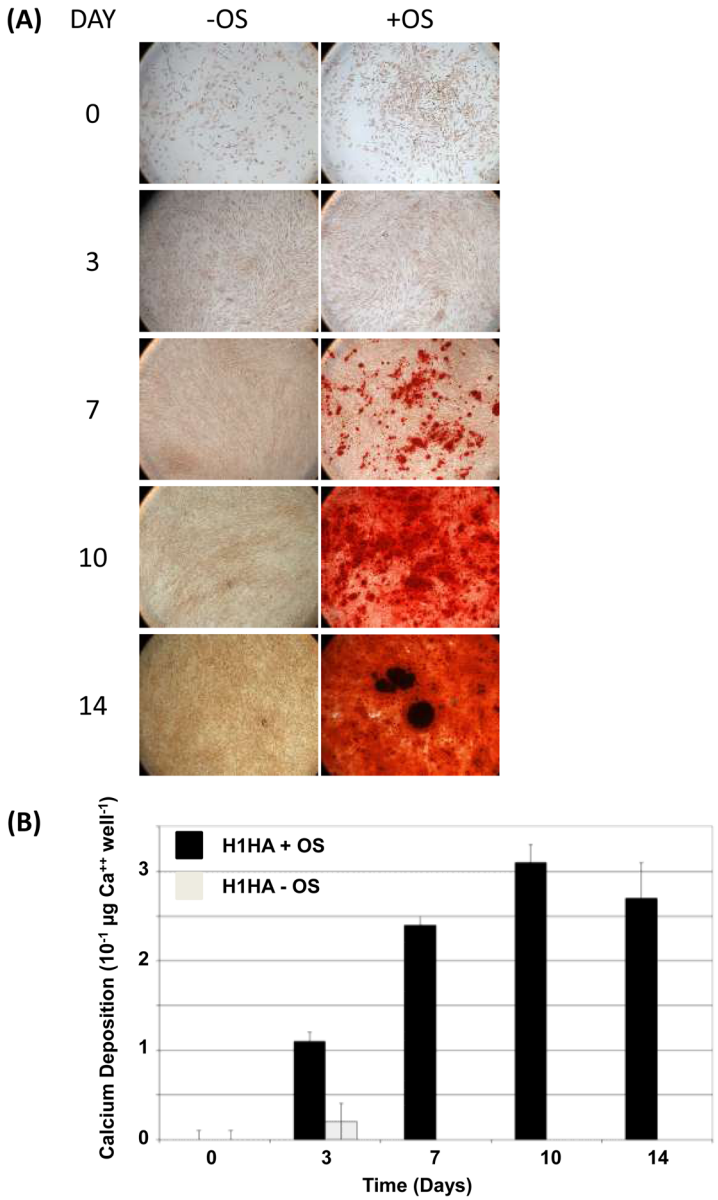

FIG. 4. Differentiation potential of hyaluronan-generated hES-derived MSC-like cells. (a) H1HA cells differentiate along the ostoeogenic lineage to form mineralised bone when cultured in conditions conducive to osteogenesis (+OS) but not control conditions (−OS), as detected by alizarin red staining (red staining detectable from day 7 onwards). (b) Calcium deposition quantified by Sigma calcium assay kit from the experiment in (a) shows that mineralised calcium only accumulates to detectable levels in osteogenic conditions (+OS, black bars).

their membrane capacitances derived using Eq. (1). The standard deviation ($\sigma = 1$) values given are based on approximating the f_{xo} and C_m distributions shown in Figure 5 as normal distributions. The results presented in Table II and Figure 5 indicate that there is a significant overlap of the membrane capacitance values for the different hESC lines, with an overall mean value of $17.6 \pm 4.7\,\text{mF/m}^2$. The overlap of the f_{xo} distributions shown in Figure 5(a) indicates that (apart from with H9) it would not be possible to obtain pure samples of different hESC lines from a mixed population using DEP as a separation tool. High purity separation of H9 cells from a mixture of H1 and H9 cells, for example, could be obtained using the DEP device described by Gupta *et al.*[13] at 120 kHz with a cell medium conductivity of 35 mS/m, but with a recovery of less than 50% for the H9 cells.

TABLE II. Summary of the data (cell diameter, DEP cross-over frequency (f_{xo}), and membrane capacitance (C_m)) obtained for the human embryonic stem cells and their differentiated progeny.

Cell type	Diameter (μm)	f_{xo} (kHz)	C_m (mF/m^2)
H1 (n = 206)	14.5 ± 2.8	68.4 ± 16.2	16.1 ± 3.9
H9 (n = 196)	11.1 ± 1.7	101.6 ± 25.8	14.2 ± 3.7
RCM1 (n = 229)	14.2 ± 2.3	68.2 ± 22	17.6 ± 6.7
RH1 (n = 254)	13.7 ± 1.6	63.8 ± 14.7	17.9 ± 3.9
T8 (n = 134)	14.3 ± 2.0	55.6 ± 13.1	20.0 ± 5.3
H1-MSC (n = 98)	15.0 ± 3.1	26.1 ± 7.4	41.6 ± 11.0
H9-MSC (n = 185)	12.5 ± 2.2	26.2 ± 7.6	49.4 ± 12.2
RCM1-trophoblast (n = 221)	12.8 ± 1.6	44.4 ± 11.8	28.3 ± 7.3

From Figure 6, it is also clear that H1 and H9 cells both exhibited well-separated distributions of their f_{xo} values, with little overlap, compared to those exhibited by their differentiated progeny (H1-MSC and H9-MSC, respectively). Separation of pure populations of differentiated cells from their progenitor H1 or H9 cells, with relatively high yields, should therefore be possible using DEP. However, DEP is unlikely to provide a sensitive method for distinguishing populations of RCM1-trophoblast from RCM1 ES cells. Coupled with the distinct separation of f_{xo} distributions after differentiation, the results shown in Figures 6 and 7 indicate that there is also a distinct increase of cellular membrane capacitance values ($p < 0.0001$). H1-MSCs and

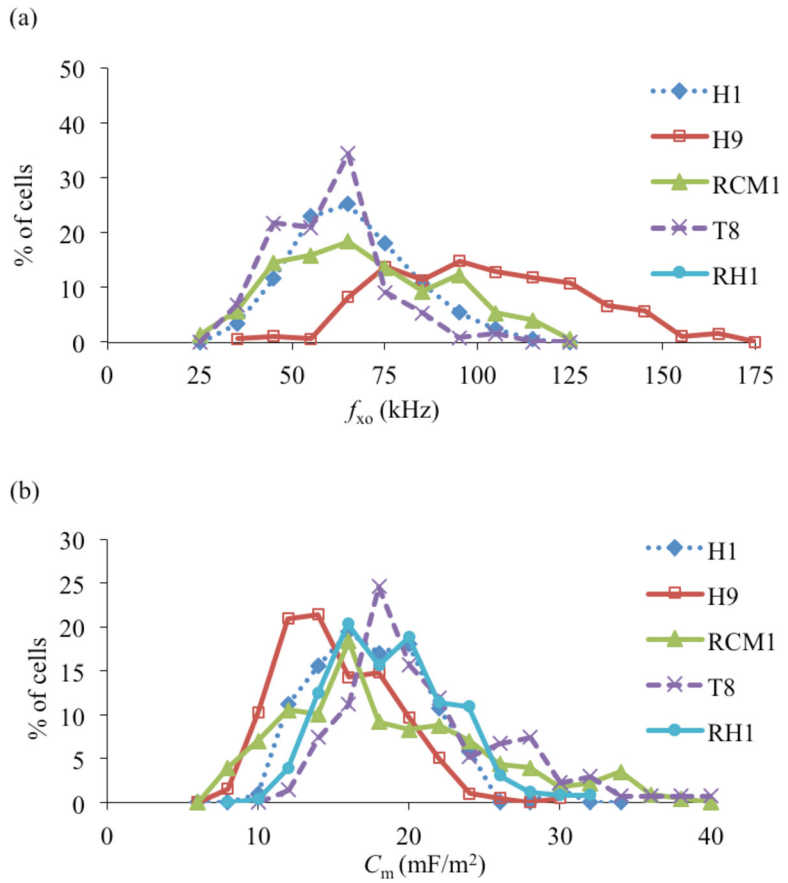

FIG. 5. (a) Percentage distributions of the DEP cross-over frequencies (f_{xo}) measured for the different human embryonic stem cell lines. (b) The derived membrane capacitance (C_m) values.

H9-MSCs exhibit a broad distribution of C_m values, extending from around 30 to 70 mF/m^2, compared to the more narrow ranges centered near 17 and 14 mF/m^2 exhibited by the H1 and H9 cells, respectively. Although the RCM1 and RCM1-trophoblast exhibit a clear difference in their mean C_m value (~18 mF/m^2 and 28 mF/m^2, respectively), there is a significant overlap of their C_m distributions. Finally, the changes in membrane capacitance and cell diameter for H9 cells as they are differentiated into H9-MSCs are shown in Figure 8 as a function of passage number. There is no statistical difference in cell diameter between H9 and H9-MSCs at passage 2 and passage 3 ($p > 0.05$). However, there is a small but significant difference in diameter when H9 cells are compared to H9-MSCs at passage numbers 4-9 ($p < 0.05$). Although the cell size increases by 12.4% from H9 to H9-MSC (p9), the observed change in the cross-over frequency can be primarily attributed to a significant increase in membrane capacitance of 247% ($p < 0.0001$).

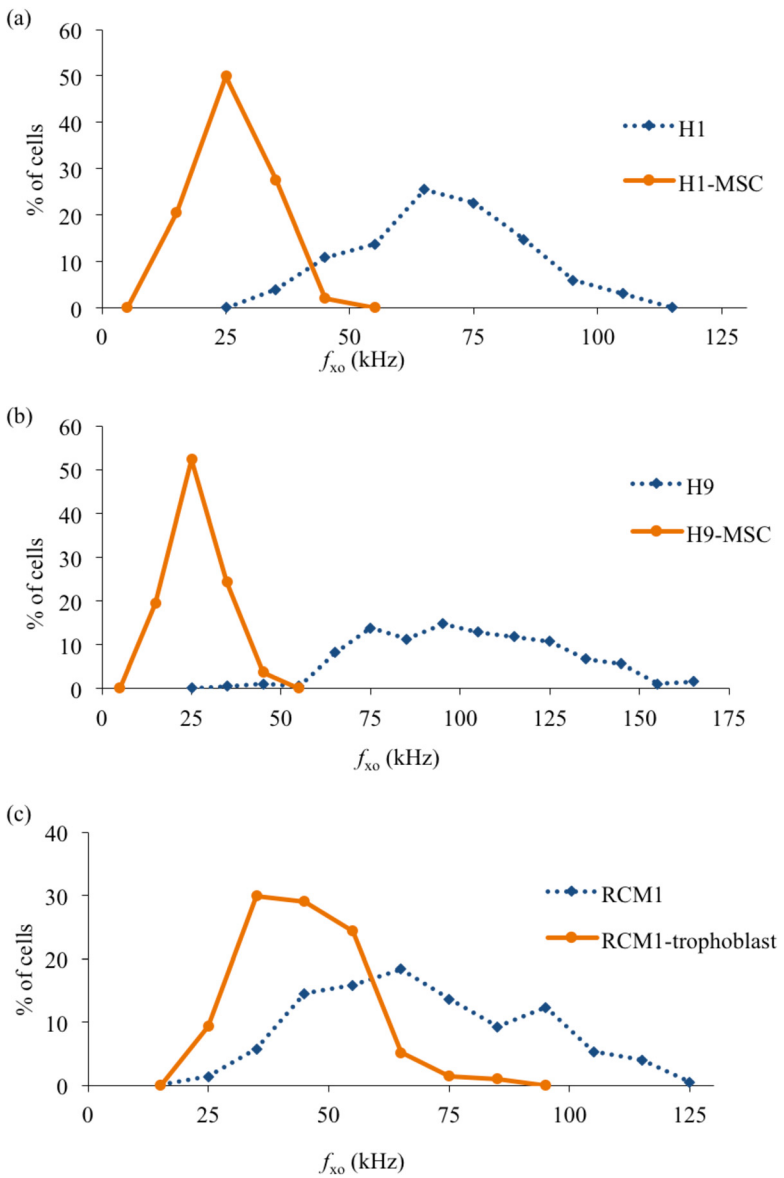

FIG. 6. Percentage distributions of the DEP cross-over frequencies (f_{xo}) for (a) H1 and differentiated H1-MSC, (b) H9 and H9-MSC, (c) RCM1 and RCM1-trophoblast.

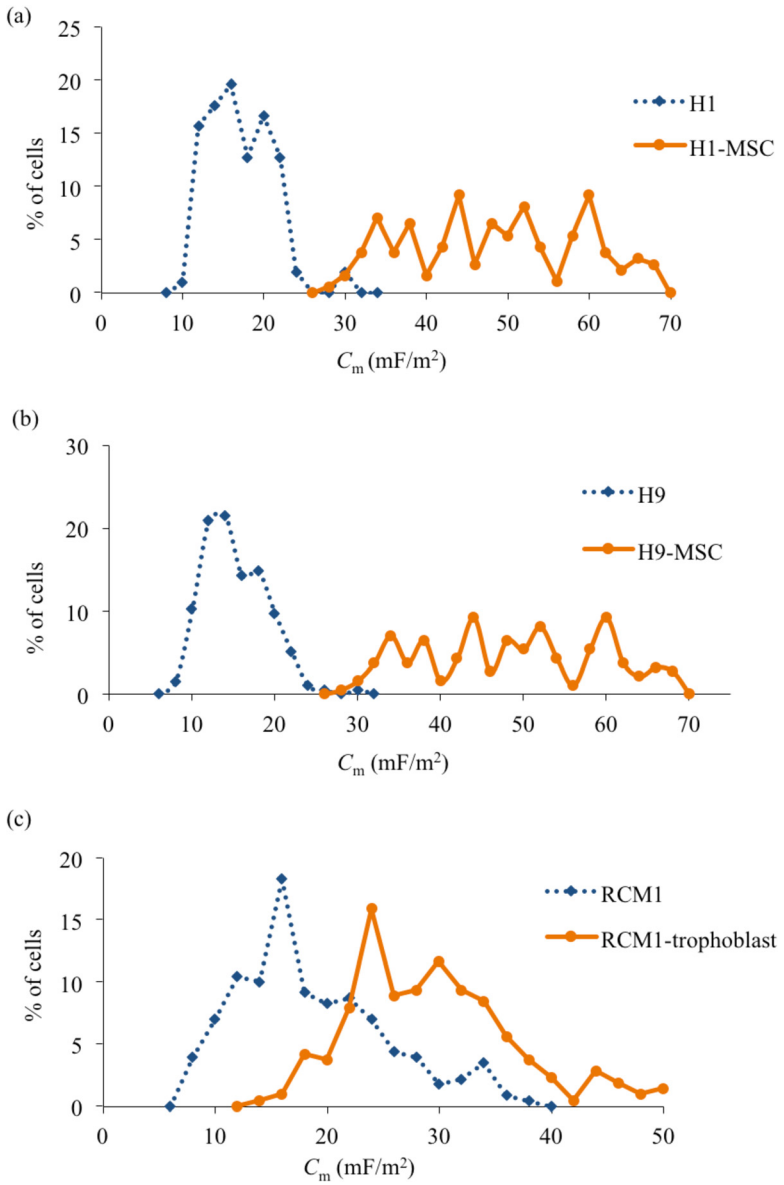

FIG. 7. Membrane capacitance (C_m) values obtained for the human embryonic stem cells and their differentiated progeny.

It is customary to employ the low-frequency (DC) approximation[25] to analyse the dielectric and conductive properties of a cell. For a spherical cell of radius r its effective permittivity ε_{eff} is given by

$$\varepsilon_{eff} = \frac{\varepsilon_o \varepsilon_m r}{\delta} \phi_m = rC_m, \tag{2}$$

where δ is the membrane thickness, ε_o the permittivity of free space, ε_m is the mean relative permittivity of the material forming the membrane structure, and ϕ_m is the membrane-folding factor to take into account cell surface features such as folds, microvilli, ruffles and blebs.[26] For a perfectly smooth spherical cell $\phi_m = 1$.

In the DEP literature,[7,14,26] it is commonly assumed that different values of C_m for different types of cell primarily reflect differences in the ϕ_m factor, and that the membrane thickness δ and relative permittivity ε_m in Eq. (2) remain relatively fixed in value (~5 nm, 2.0–2.2, respectively[26,27]). However, recent DEP determination of C_m for fibroblasts and myoblasts, combined

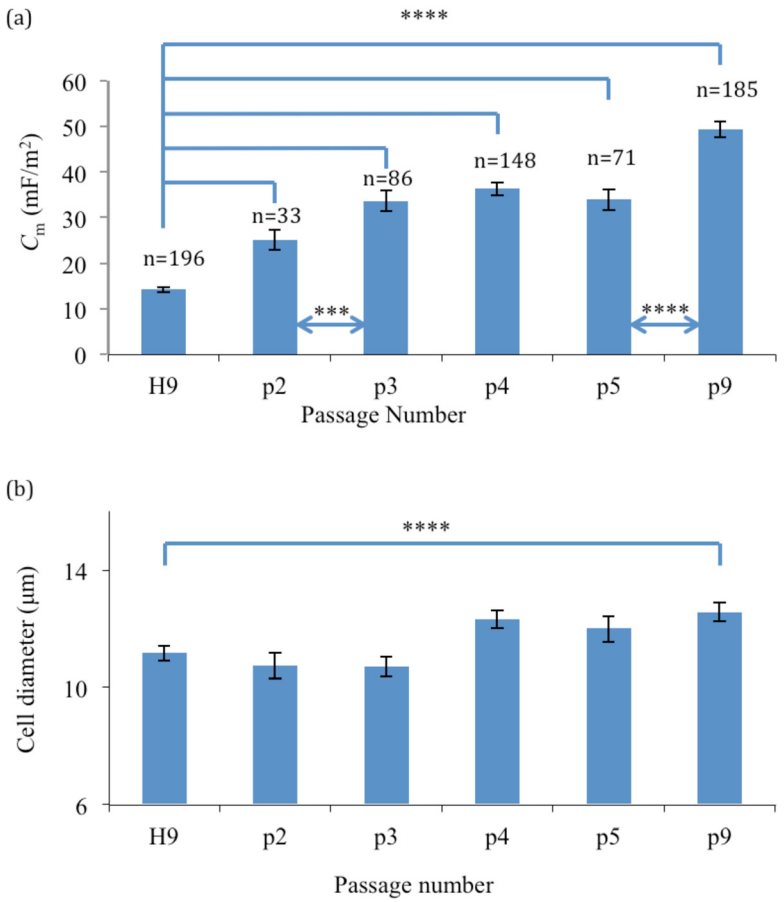

FIG. 8. The progression of (a) mean membrane capacitance C_m with 95% confidence interval bars, and (b) mean cell diameter with 95% confidence interval error and passage number for the H9 cells cultured on an hyaluronan coated substrate. (**** and *** signify a statistical difference with $p < 0.0001$ and $p < 0.001$ between groups).

with Raman spectroscopic analyses of their membranes, has indicated that the chemical composition (e.g., proportion of saturated to unsaturated lipid content) may have a greater influence on the values for δ and ε_m than previously thought.[28]

Our study supports further development of DEP in the context of human embryonic stem cell bioprocessing, in the course of expansion or directed differentiation for industrial or therapeutic applications. The most tractable application would be for purposes of real-time monitoring of the representation of specific cell subpopulations through sampling limited quantities of cells at the time of passaging. This would not require large numbers of cells and could be implemented essentially using methods applied in this study. The application of DEP to the separation of relatively large numbers of cells (>50 000) has been previously demonstrated (e.g., Refs. 13 and 28). Scaled separation of tissue derived stem cells and differentiated progeny for further culture by such approaches will require process parallelization.

IV. CONCLUSIONS

The various undifferentiated hESC lines (H1, H9, RCM1, RH1) and the transgenic clonal derivative (T8) studied in this work could not be discriminated in terms of their DEP cross-over frequencies and derived membrane capacitance values (14–20 mF/m^2). However, the differentiated progeny (H1-MSC, H9-MSC, RCM1-trophoblast) could be discriminated from their adult precursors (H1, H9, RCM1, respectively) by significant increases in their mean DEP cross-over frequencies and derived membrane capacitance values. The mesenchymal stem cell-like phenotypes (H1-MSC, H9-MSC) derived from differentiation of H1 and H9 exhibited

comparable C_m values of 41–49 mF/m^2 ($p < 0.0001$), whereas induction of RCM1 to a trophoblast cell-like phenotype resulted in a smaller increase of mean C_m values from 17.6 to 28.3 mF/m^2 ($p < 0.0001$). Since different hESC lines were derived at different times in different laboratories, and have been cultured in different conditions at different times, yet C_m and f_{xo} are similar, we conclude that a low membrane capacitance is a characteristic property of hESCs. Furthermore, the result that C_m changes upon differentiation suggests that different phenotypes might be discriminated by their C_m values. The transition to a larger membrane capacitance as the H9 cells differentiated to H9-MSCs was progressively evident after each passage of the cell culture up to p9 (Figure 8). All of these findings confirm the existence of distinctive parameters which differ between undifferentiated and differentiating hESCs, and suggests that dielectrophoresis can be applied in the manufacturing process of these cells.

The increase in membrane capacitance during differentiation could arise from an increase in the complexity of the membrane surface (appearance of folds, microvilli, blebs), or a combined thinning and increase of the effective dielectric polarisability of the membrane structure.[28] Which of these physico-chemical parameters contributes the most to the observed changes of membrane capacitance remains a focus of our ongoing studies.

ACKNOWLEDGMENTS

The authors would like to thank associates for their technical assistance. Notably Mrs. Judy Fletcher and Ms. Davina Wojtacha for osteogenic differentiation and assessment of calcium deposition; Ms. Courtney Campbell for *in situ* immunocytochemistry; and Dr. Paz Freile for flow cytometry. This work was supported by EUFP7 funding to P.D.S., as part of a HEALTH-2007-1.4-10 7 program to develop stem cell culture conditions (Project No. 223410), and by funding to R.P. by the Edinburgh Research Partnership in Engineering and Mathematics.

[1]J. A. Thomson, J. I. Eldor, S. S. Shapiro, M. A. Waknitz, J. J. Swiergiel, V. S. Marshall, and J. M. Jones, Science **282**, 1145 (1998).
[2]I. Klimanskaya, Y. Chung, S. Becker, S. J. Lu, and R. Lanza, Nature **444**, 481 (2006).
[3]K. Takahashi and S. Yamanaka, Cell **126**, 663 (2006).
[4]Z. R. Gagnon, Electrophoresis **32**, 2466 (2011).
[5]B. Çetin and D. Li, Electrophoresis **32**, 2410 (2011).
[6]J. Regtmeier, R. Eichhorn, M. Viefhues, L. Bogunovic, and D. Anselmetti, Electrophoresis **32**, 2253 (2011).
[7]R. Pethig, Biomicrofluidics **4**, 022811 (2010).
[8]M. S. Talary, K. I. Mills, T. Hoy, A. K. Burnett, and R. Pethig, Med. Biol. Eng. Comput. **33**, 235 (1995).
[9]M. Stephens, M. S. Talary, R. Pethig, A. K. Burnett, and K. I. Mills, Bone Marrow Transplant. **18**, 777 (1996), available online at http://www.ncbi.nlm.nih.gov/pubmed/8899194/.
[10]J. Vykoukal, D. M. Vykoukal, S. Freyberg, E. U. Alt, and P. R. C. Gascoyne, Lab Chip **8**, 1386 (2008).
[11]L. A. Flanagan, J. Lu, L. Wang, S. A. Marchenko, N. L. Jeon, A. P. Lee, and E. S. Monuki, Stem Cells **26**, 656 (2008).
[12]F. H. Labeed, J. Lu, H. J. Mulhall, S. A. Marchenko, K. F. Hoettges, L. C. Estrada, A. P. Lee, M. P. Hughes, and L. A. Flanagan, PLoS ONE **6**(9), e25458 (2011).
[13]V. Gupta, I. Jafferji, M. Garza, V. O. Melnikova, D. K. Hasegawa, R. Pethig, and D. W. Davis, Biomicrofluidics **6**, 024133 (2012).
[14]X. Wang, F. F. Becker, and P. R. C. Gascoyne, Biochim. Biophys. Acta **1564**, 412 (2002).
[15]R. Pethig, V. Bressler, C. Carswell-Crumpton, Y. Chen, L. Foster-Haje, M. E. García-Ojeda, R. S. Lee, G. M. Lock, M. S. Talary, and K. M. Tate, Electrophoresis **23**, 2057 (2002).
[16]R. Pethig and M. S. Talary, IET Nanobiotechnol. **1**, 2 (2007).
[17]A. C. Sabuncu, J. Zhuang, J. F. Kolb, and A. Beskok, Biomicrofluidics **6**, 034103 (2012).
[18]P. A. De Sousa, J. Gardner, S. Sneddon, S. Pells, B. J. Tye, P. Dand, D. M. Collins, K. Stewart, L. Shaw, S. Przyborski, M. Cooke, K. J. McLaughlin, S. J. Kimber, B. A. Lieberman, I. Wilmut, and D. R. Brison, Stem Cell Res. **2**, 188 (2009).
[19]J. M. Fletcher, P. M. Ferrier, J. O. Gardner, L. Harkness, S. Dhanjal, P. Serhal, J. Harper, J. Delhanty, D. G. Brownstein, Y. R. Prasad, J. Lebkowski, R. Mandalam, I. Wilmut, and P. A. De Sousa, Cloning Stem Cells **8**, 319 (2006).
[20]L. Gerrard, D. Zhao, A. J. Clark, and W. Cui, Stem Cells **23**, 124 (2005).
[21]L. Harkness, A. Mahmood, N. Ditzel, B. M. Abdallah, J. V. Nygaard, and M. Kassem, Bone **48**, 231 (2011).
[22]R.-H. Xu, X. Chen, D. S. Li, R. Li, G. C. Addicks, C. Glennon, T. P. Zwaka, and J. A. Thomson, Nat. Biotechnol. **20**, 1261 (2002).
[23]J. Kapuściński and B. Skoczylas, Nucleic Acids Res. **5**(10), 3775 (1978).
[24]V. Sottile, A. Thomson, and J. McWhir, Cloning Stem Cells **5**, 149–155 (2003).
[25]H. P. Schwan, Adv. Biol. Med. Phys. **5**, 147 (1957), available online at http://www.ncbi.nlm.nih.gov/pubmed/13520431?dopt=Citation.
[26]X. B. Wang, Y. Huang, P. R. Gascoyne, F. F. Becker, R. Holzel, and R. Pethig, Biochim. Biophys. Acta **1193**(2), 330 (1994).
[27]R. Pethig and D. B. Kell, Phys. Med. Biol. **32**, 933 (1987).
[28]M. Muratore, V. Srsen, M. Waterfall, A. Downes, and R. Pethig, Biomicrofluidics **6**, 034113 (2012).